ELSEVIER

Carbohydrate Polymers 45 (2001) 385–393

Carbohydrate Polymers

www.elsevier.com/locate/carbpol

CoSalen immobilized to chitosan and its electrochemical behavior

D.D. Hu[a], Q.Z. Shi[a], Z.X. Tang[a], Y. Fang[b], J.F. Kennedy[c,*]

[a]*Chemistry Department of Northwest University, Xi'an 710069, People's Republic of China*
[b]*Chemistry Department of Shaanxi Normal University, Xi'an 710062, People's Republic of China*
[c]*School of Chemistry, University of Birmingham Research Park, Birmingham B15 2SQ, UK*

Received 14 January 2000; revised 19 June 2000; accepted 19 June 2000

Abstract

A chitosan (CS) immobilized cobalt complex (CS–CoSalen) was prepared by immersing a CS film into the saturated aqueous solution of a cobalt(II) complex of *N*,*N*′-bis(salicylaldehyde)ethylenediimino (CoSalen). The CS–CoSalen was characterized, and it was found that CoSalen was immobilized onto CS through the coordination of the amino group of CS. The cobalt(II) ion in the CS–CoSalen has a five-coordination structure. Its vacant sixth coordination site was found to bind molecular oxygen reversibly. Electrochemical studies demonstrated that the CS–CoSalen is active for the catalysis of the electrochemical reduction of oxygen to hydrogen peroxide in an aqueous medium. © 2001 Elsevier Science Ltd. All rights reserved.

Keywords: Chitosan; Electrochemical behavior; Cobalt(II) complex

1. Introduction

Earlier studies of cobalt complexes were concerned primarily with the synthesis, structure, electronic, magnetic, and other characteristic studies of the complexes (Smith & Pilbrow, 1981). More recently, the literature reveals considerable interest in the potential applications of cobalt complexes. Among these, most are concerned with the ability of cobalt(II) complexes to interact with dioxygen. These complexes have been used as models to mimic oxidases that activate dioxygen in the oxidation of organic substrates (Rindone, 1985; Ruzie, Smith & Pilbrow, 1982). Studies on the use of cobalt complexes immobilized as films or cells for the separation of oxygen from air were also carried out (Drago, Gaul, Zombec & Strub, 1980). To prevent the formation of μ-oxo-dimers, which are inactive for the activation of molecular oxygen, Bied-charreton, Frostin-rio, and Gaudemer (1982) and others studied in some detail the synthesis and properties of polymer-supported cobalt complexes. Although many advantages can be foreseen for these polymer-supported complexes, they may not be suitable for biological or food applications because they are not biodegradable or blood-compatible. Unlike synthetic polymers, chitosan (CS) is biodegradable (Knorr, 1987) and blood-compatible. In fact, CS has recently been used in the food industry, in processing drinking water, and in several biomedical applications (Yang & Vigee, 1991). It also has been used as a carrier for immobilizing cells (Leuba et al., 1979).

Considering the fact that the CoSalen complex is active for the activation of molecular oxygen and the complex is easily deactivated due to formation of μ-oxo-dimers, (Mark, Carter, Paul & Fred, 1974), a CS-supported CoSalen was prepared and characterized. Furthermore, its electrochemical behavior was also investigated by employing voltammetry. To our knowledge, no information is available to date on this immobilized complex. This paper reports the results from this study.

2. Materials and methods

2.1. Materials

CS was prepared by deacetylation of chitin by using a previously reported method (Midorigaoka, 1983). Several methods, including thermal analysis, infrared spectroscopy and elemental analysis, have been employed for the characterization of the product. The peak at 1655 cm^{-1} in the profile of the IR spectrum of chitin became insignificant after deacetylation, clear evidence for the formation of CS (Midorigaoka, 1983). The thermal analysis (DTG–TG) indicates that the decomposition behavior of the product was in agreement with the literature (Peniche-Covas &

---

[*] Corresponding author. Tel.: +44-121-414-7029; fax: +44-121-414-7030.

E-mail address: jfkennedy@chemistry.bham.ac.uk (J.F. Kennedy).

0144-8617/01/$ - see front matter
PII: S0144-8617(00)00267-8

Table 1
Data of elemental analysis for CoSalen

Elements	Found	Calculated
C%	58.93	59.10
H%	4.32	4.31
N%	8.50	8.62
Co%	17.97	18.13

Jimenez, 1988). The degree of deacetylation of the sample was determined by potentiometric titration (Ke & Chen, 1990), and was found to be 100%. The intrinsic viscosity of CS was determined in 0.2 M acetic–0.1 M sodium chloride at 25°C with an Ubbelohde-type viscometer. The viscosity-average-molecular weight ($\bar{W}_v$) of CS was calculated according to the following equation

$$[\eta] = 2.51 \times 10^{-5} \bar{W}_v^{0.87}$$

The viscosity-average-molecular weight ($\bar{W}_v$) was determined to be 7.86×10^5. The product fits the formula $C_6H_{11}O_4N{\cdot}0.83H_2O$. Other chemicals were of reagent grade and were used without further purification.

CoSalen was prepared by employing a method described in the literature (Matsujiro, 1980). 0.6 g of ethylenediamine was added to 50 ml of ethanol solution containing 2.44 g of salicylaldehyde under stirring. After the solution was stirred for approximately 15 min, a yellow product, H_2Salen, precipitated. The reaction mixture was heated, until the precipitate was dissolved. A solution containing 2.49 g of $CoAc_2{\cdot}4H_2O$ in (15 ml of ethanol was prepared and mixed with the H_2Salen solution. The mixture was refluxed for 2 h and then cooled to room temperature. The CoSalen was filtered and washed with ethanol. Reddish brown microcrystals were obtained after drying under vacuum at 100°C. The elemental analysis results are shown in Table 1. The compound fits a formula of $C_{16}H_{14}O_2N_2Co$. The characteristic peak, which appeared at 1625 cm^{-1} in the profile of the IR spectrum of CoSalen, is assigned to ν(C=N).

The CS–CoSalen was prepared in the following way. CS (2.0 g) was dissolved in a dilute acetic acid solution (1.0%, 114 ml) resulting in a viscous transparent solution. The solution was carefully cast on a glass plate, dried at room temperature for 5 h, and then dried in vacuum at 120°C for 4 h. The plate was immersed in NaOH solution ($C = 1$ mol l^{-1}) for 2 h, then washed with pure water until neutrality. A transparent and flexible CS membrane was delaminated from the plate after drying in vacuum at 120°C for 4 h. The membrane was cut into a sheet of 1 cm^2. The membrane obtained thereby was placed in a saturated aqueous solution of CoSalen (20 ml) for 12 h, then washed with pure water several times. A light brown membrane of CS–CoSalen was obtained after drying in vacuum at 120°C for 5 h.

A glassy carbon electrode (GCE) (5 mm in diameter) covered with a teflon tube was polished with alumina (4.05 μm diameter particles). After being washed with water and dried at 120°C for 2 h, the polished surface was coated with an aqueous solution of CS (1.7%, containing 1.0% acetic acid, 20 ml), dried at room temperature for 2 h, and then dried in vacuum at 120°C for 2 h. The electrode was immersed in NaOH solution ($C = 1$ mol l^{-1}) for 1.5 h, and washed with pure water until neutrality. Thus, a CS-modified electrode was obtained after further drying in vacuum at 120°C for 2 h. The CS-modified electrode was immersed in the saturated aqueous solution of CoSalen (20 ml) at room temperature for 24 h. After this treatment, the electrode was washed with plenty of water and stored in KCl solution (0.1 mol l^{-1}).

2.2. Methods

2.2.1. IR spectrometry

The IR spectra were recorded on a Mattson FT-IR spectrophotometer, as a KBr disc for CoSalen and as films for CS and CS–CoSalen, respectively.

2.2.2. UV–VIS spectrometry

The UV–VIS spectra were recorded on a spectrophotometer (Mold, 756 MC) with an appropriate quartz cell for CoSalen solution in $CHCl_3$, and membranes for CS and CS–CoSalen, respectively.

2.2.3. Electron spin resonance spectrometry

The ESR spectra were taken on a Varian-E109 operating at the X-band frequency and at room temperature for CoSalen, CS and CS–CoSalen, respectively. Tetracyanoquinodimethane was used as an external standard ($g = 2.0026$).

2.2.4. X-ray photoelectron spectrometry

The XPS spectra were determined using a Perkin–Elmer PHI-5400 photoelectrometer. Binding energy of C_{1s} was used as an external standard. XPS spectra were deconvoluted using the GASCAPIV program. The program requires input for the number of peaks and the half-width, and position for each peak suspected of comprising the multiplet. Based on these parameters, a spectrum is calculated, which can be compared to the experimental spectrum. The program contains a routine that performs a point-by-point subtraction of the calculated spectrum from the experimental spectrum, until the calculated spectrum from the deconvoluted spectra fits the experimental spectrum very well.

2.2.5. Analysis of composition

The contents of C, H, N in CoSalen, CS and CS–CoSalen were determined with a Perkin–Elmer 2400 analyzer. Cobalt was determined with an atomic absorption spectrophotometer (WFX-IF 2).

2.2.6. Electrochemical study

The electrochemical behavior of the CS-supported

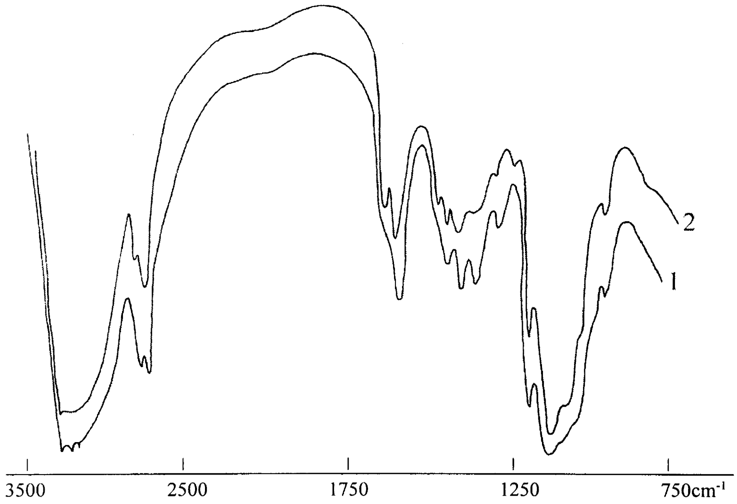

Fig. 1. IR spectra of: (1) CS; and (2) CS–CoSalen.

complex was investigated using the following instruments and method. Cyclic voltammetry was performed at room temperature with a DJS-292 Model Potentiostat, XFD-8B ultra-low-frequency signal generator and ultra-low-frequency oscillograph. A conventional single-compartment cell, equipped with a three-electrode configuration, was employed. All measurements were performed in solution (0.1 mol l^{-1} KCl). The CS–CoSalen-treated electrode was used as working electrode. A saturated calomel electrode was used as a reference electrode (SCE), and a sheet of platinum as counter-electrode. The potentials shown in the cyclic voltammetry curve vs. SCE, E_{pa} and E_{pc} are the potentials of anodic oxidation and cathodic reduction, respectively. The half-wave potential was calculated using $E_f = 1/2(E_{pa} - E_{pc})$.

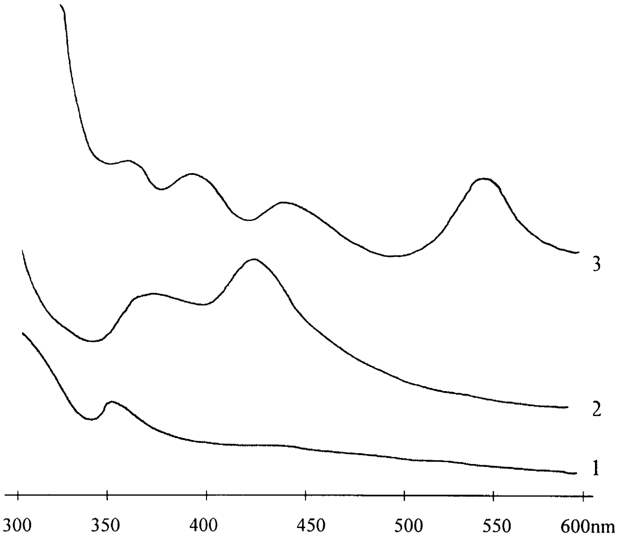

Fig. 2. UV-VIS spectra of: (1) CS; (2) CoSalen; and (3) CS–CoSalen.

3. Results and discussion

3.1. Spectrometric study

The IR spectra of the CS and CS–CoSalen films are shown in Fig. 1. It can be seen that the profiles for the CS differ from those for the CS–CoSalen complex. A broad band at 3360 cm^{-1}, with small sharp peaks, corresponds to ν_{as}(H–N–H) and ν_{sym}(H–N–H) of CS, whereas the corresponding band in the CS–CoSalen spectrum shifts to a low-frequency region, 3360–3000 cm^{-1}. The peak corresponding to $\nu(NH_2)$ in the spectrum of CS shifts to 1600 cm^{-1} after CoSalen was immobilized. The reasons for these changes can be attributed to the coordination of the amino group of CS to cobalt in CoSalen. The fact that the ν_{as}(H–N–H) and ν_{sym}(H–N–H) shift to a low-frequency region may originate from the electronic charge transfer from nitrogen to cobalt. The interaction between the amino group and cobalt may affect the vibration of δ(H–N–H) by stereo-hindrance. Thus, the peak of δ(H–N–H) shifts to a higher wave number. The appearance of a new peak at 1645 cm^{-1} in the spectrum of CS–CoSalen may be attributed to ν(C=N) of CoSalen. Additionally, the appearance of a band at 1205 cm^{-1} in the spectrum of CS–CoSalen exposed to oxygen may correspond to the absorption of ν(O–O), which relates to the $Co–O_2^-$ (Dai, Li & Han, 1988). The IR results indicate that as an axial donor, the amino groups of CS may be coordinated to the cobalt of CoSalen, and this immobilized complex can absorb oxygen to form a six-coordinate structure complex.

The electronic spectra of CoSalen in $CHCl_3$, CS and CS–CoSalen films are shown in Fig. 2. CoSalen is known to be a four-coordinate Co(II) complex in $CHCl_3$ (Robert et al., 1979). Absorption bands at 350 and 410 nm are assigned to n–π^* transition of the ligand and to d–d transition of the central ion, respectively, whereas, in the case of the

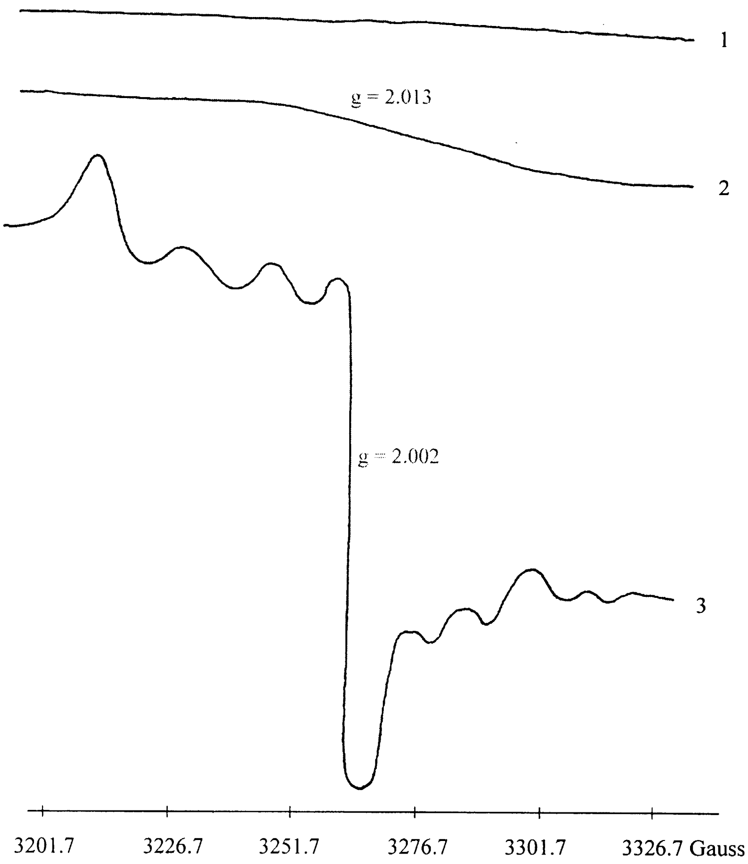

Fig. 3. ESR spectra of: (1) CS, (2) CoSalen, and (3) CS–CoSalen.

CS–CoSalen films, the corresponding peaks of absorption appear at 375 and 425 nm, respectively. These peaks are red-shifted in comparison with that of CoSalen. The reasons for these changes can be attributed to the coordination of the NH_2 group of CS to the central ion, cobalt, which makes the electronic density of the equatorial plane conjugates system increase. This result is reasonably interpreted by Goutermen's theory (Mark et al., 1974). A new band appearing in the range of 500–600 nm may be assigned to the absorption of an oxygen adduct (CS–CoSalen–O_2) (Tsuchida, Nishide & Ohyanagi, 1987).

Electron spin resonance spectroscopy provides a very sensitive probe for the existence of low-spin Co(II) and of superoxo-cobalt(II) centers. The dioxygen adducts give rise to a characteristic ESR signal at about $g = 2$. Any peroxo-bridged dimers of type $(CoSalen)_2O_2$ will, of course, be ESR silent. Some typical ESR spectra of CoSalen, CS and CS–CoSalen are shown in Fig. 3. The CoSalen gives a very

Table 2
XPS data on Chitosan(CS), CoSalen and CS–CoSalen (Eb/eV)

	N_{1s}	$Co_{2p3/2}$	O_{1s}
CS	399.2		532.2, 533.02
CoSalen	399.4	780.8	530.9
CS–CoSalen	399.23, 35,401.45	781.5	530.82, 532.24, 533.05

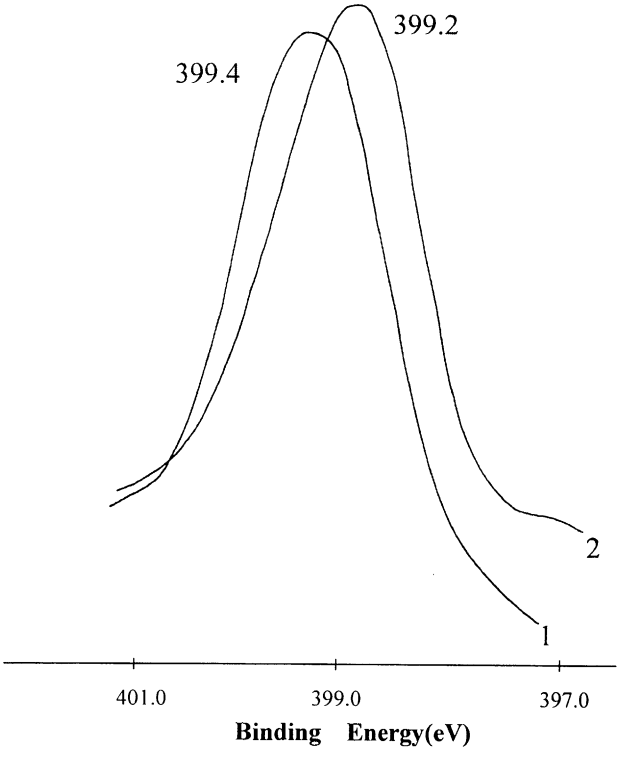

Fig. 4. N_{1s} XPS spectra of: (1) CS membrane; and (2) CoSalen.

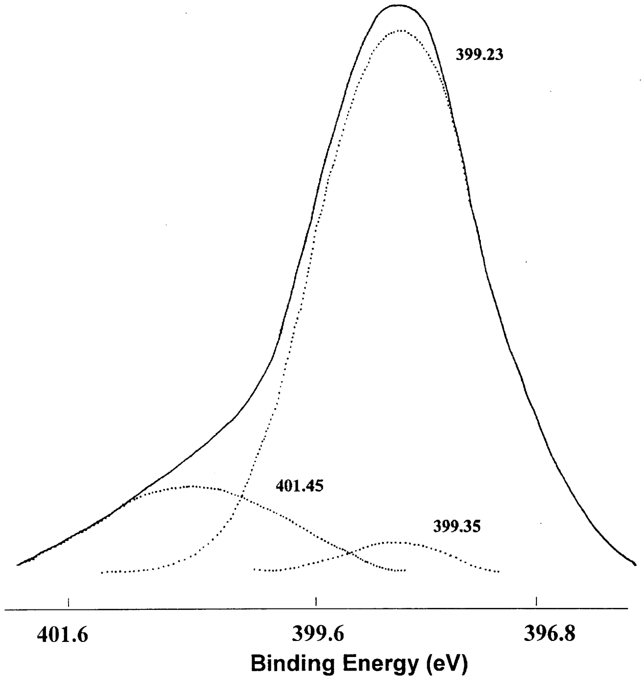

Fig. 5. N_{1s} XPS spectrum of CS–CoSalen and its deconvoluted spectra.

broad, poorly resolved signal. A clear signal at $g = 2.002$ appears in the ESR spectrum of the CS–CoSalen complex. This indicates that there is a superoxo-Co(III) moiety in the CS–CoSalen or an axial donor coordinate to cobalt of CoSalen, or that both coexist (Busetto, Cariati & Fusi, 1973; Murray, Van den Bergen & Kennedy, 1986; Sakurada, 1980), namely, the cobalt ion in the CS–CoSalen possesses a six-coordinate structure, and molecular oxygen binds to the CS–CoSalen through its vacant sixth coordination site. Additionally, a series of clear superhyperfine splitting lines are observed in the ESR spectrum of the CS–CoSalen complex ($A = 17.3$ Gauss). The splitting lines are attributed to the stronger interaction between CS and CoSalen. It is for this reason that the coupling between the cobalt nucleus ($l = 7/2$, $N = 8$) and its single electron becomes clear, appearing as eight superhyperfine splitting lines. The values of g and A are in accordance with those reported by Diemente, Hoffman, and Basolo (1970) ($g = 1.997$, $A = 17.9$ Gauss) for a polymer immobilized cobalt complex to possess a six-coordinate structure.

To further our study of coordination between CS and CoSalen, CS, CoSalen and CS–CoSalen have been characterized by X-ray photoelectron spectroscopy. The results are listed in Table 2 and shown in Figs. 4 and 5, respectively.

N_{1s} binding energies for CS and CoSalen are 399.2 and 399.4 eV, respectively, as shown in Fig. 4. The $N_{1s1/2}$ signal from the CS–CoSalen complex was complicated by the presence of several different types of nitrogen in it. In order to separate the individual peaks comprising the broad signal, the $N_{1s1/2}$ signal from the CS–CoSalen complex was deconvoluted. The deconvolution results are shown in Fig. 5. The fit between calculated and experimental peaks is quite good. The peaks that comprise the calculated spectrum were plotted individually in Fig. 5, and the binding energies associated with these peaks are listed in Table 2. The peak at 399.35 eV was assigned to the $N_{1s1/2}$ of CoSalen in CS–CoSalen, which is almost unchanged in comparison with that of unimmobilized CoSalen, whereas the $N_{1s1/2}$ peak at 401.45 eV is greater than that of CS. These results are not difficult to understand because the peaks at 399.23 and 401.45 eV are, respectively, assigned to the nitrogen atoms in unreacted and reacted amino groups of CS by a comprehensive consideration of the $N_{1s1/2}$ binding energy and its intensity. The binding energy of 401.45 eV is significantly larger than that of CS. Clearly, the greater binding energy may be attributed to nitrogen atoms, which are in coordination to cobalt in CoSalen.

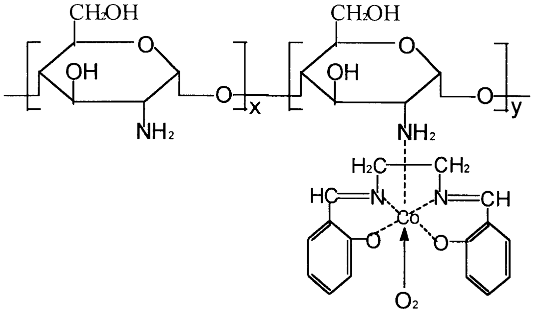

Fig. 6. Proposed structure of CS–CoSalen.

The XPS data of $Co_{2p3/2}$ are presented in Table 2. The $Co_{2p3/2}$ binding energy is 780.8 eV for CoSalen, whereas that for CS–CoSalen is 781.5 eV. The fact that the nitrogen in CS coordinates to the cobalt in CoSalen may increase the electron density on cobalt by donation of a lone electron pair. The increase in electron density may result in a lower cobalt binding energy, rather than a higher one. This apparent contradiction may be explained by the fact that the five-coordinate CS–CoSalen is a high-spin complex, whereas the four-coordinate one is a low-spin complex. The nucleus of the metal is more "shielded" from some of the electron density of the ligand in the high-spin form than in the low-spin form due to metal–ligand electron–electron repulsion. Consequently, the positive charge on the metal ion is not reduced as much as it would be if the complex were low-spin, and the binding energy for the central ion is higher (Burness, Dillard & Taylor, 1975).

The XPS data of $O_{1s1/2}$ are listed in Table 2. A broad peak for $O_{1s1/2}$ of the CS–CoSalen complex was deconvoluted into three narrower peaks. Each of the narrower peaks was identified by comparison of the $O_{1s1/2}$ binding energies and intensity for CS, CoSalen and the CS–CoSalen. The binding energies of $O_{1s1/2}$ in CS and CoSalen are basically unchanged. This shows that the oxygen atoms of CS may not take part in the coordination to CoSalen. It is to be noted that the XPS spectra for all samples were determined under vacuum conditions. This means that there is no oxygen binding in the sample.

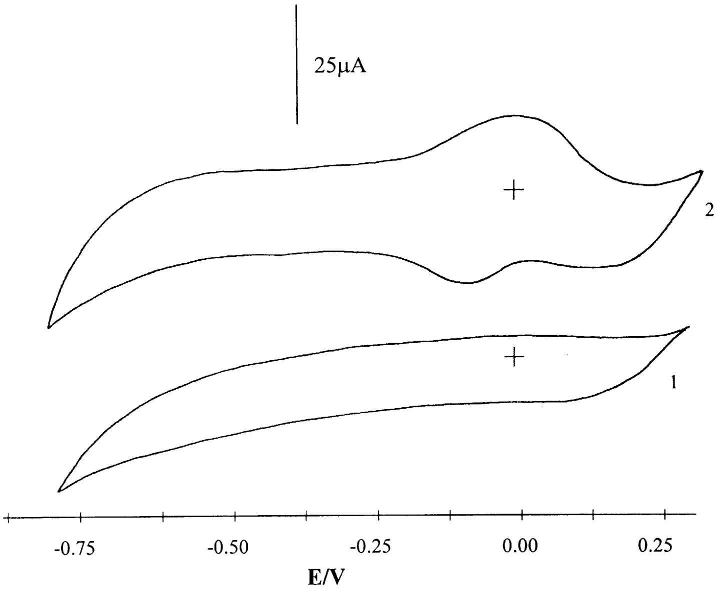

Fig. 7. Cyclic voltammograms of the GCE modified by: (1) CS; and (2) CS–CoSalen in the aqueous solution of KCl (0.1 mol l^{-1}). Measuring condition: N_2 atmosphere, sweep rate: 25 mV/s.

The composition of CS–CoSalen was determined by elemental analysis. It fits the formula (monomer of CS)$_1$: (CoSalen)$_{0.23}$.

Assembling all the characterized information on the CS–CoSalen complex together indicates that CoSalen was immobilized onto CS through coordination of the amino group in CS to the cobalt in CoSalen. The sixth coordination site of the CS–CoSalen complex may be occupied by molecular oxygen when it is exposed to air. A proposed structure for CS–CoSalen is shown in Fig. 6.

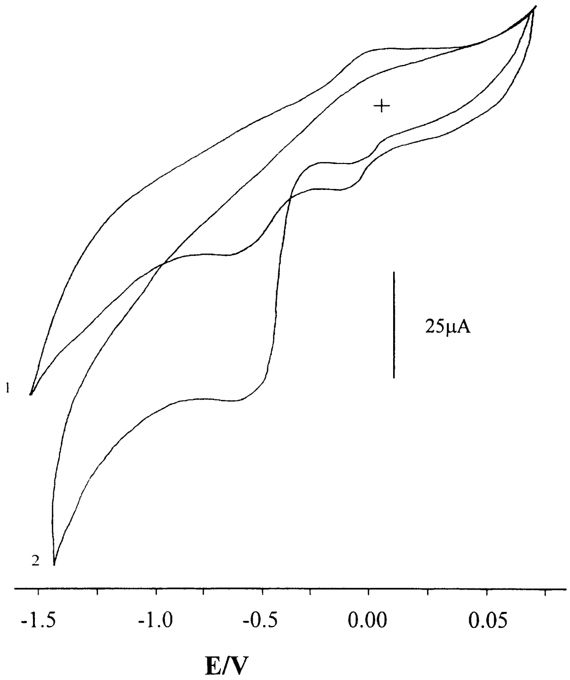

Fig. 8. Cyclic voltammograms of the GCE modified by CS–CoSalen measured under N_2 atmosphere and at different scan rates: (1) 250; and (2) 25 mV/s (the electrode was exposed to air for 30 min before it was immersed in 0.1 mol l^{-1} KCl solution).

3.2. Electrochemical study

The cyclic voltammogram of the CS-modified GCS in KCl solution (0.1 mol l^{-1}) under N_2 atmosphere was recorded and the results are shown in Fig. 7(1). It can be seen that there are no significant waves in the curve. However, two peaks appeared in the cyclic voltammogram of the CS–CoSalen-modified electrode (Fig. 7(2)). The one appearing at 0 V is an oxidation peak, the other appearing at −0.053 V is a reduction peak. Both peaks are reversible upon repetitive cycling. These results indicate that the CS–CoSalen-modified electrode is electrochemically active. The oxidation–reduction waves may correspond to the reaction shown in Eq. (1).

$$\text{CS–Co(II)Salen} \underset{+e}{\overset{-e}{\rightleftharpoons}} \text{CS–Co(III)Salen} \qquad (1)$$

The cyclic voltammogram obtained by a quick scan (250 mV/s) of the CS–CoSalen-modified electrode is shown in Fig. 8(1). It is to be noted that the electrode was exposed to air for 30 min before it was immersed in KCl solution (0.1 mol l^{-1}) for electrochemical measurement. Clearly, the profile is very different from that of Fig. 7(2). The oxidation potential at 0 V is unchanged, whereas the peak current decreased, and the reduction peak at −0.053 V disappeared. Two new reduction peaks appeared at −0.23 and −0.67 V, respectively. The cyclic voltammogram was gradually restored to the previous profile when nitrogen was blown into the solution for 20–30 min. The reduction peaks at −0.23 and −0.67 V appeared again, when oxygen was

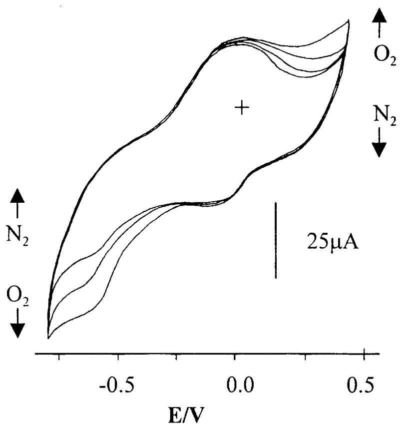

Fig. 9. The reversible changes of the cyclic voltammogram of the GCE modified by CS–CoSalen upon alternate bubbling of O_2 and N_2 through the aqueous solution of KCl (0.1 mol l^{-1}). Scan rate: 250 mV/s.

blown into the solution for a few minutes. Furthermore, the peak currents increased with increase in gas-bubbling time (Fig. 9). These results indicate that the CS–CoSalen-modified electrode could reversibly bind oxygen. This conclusion is reasonable, considering the structure of the complex. In order to confirm this, IR spectra of the CS–CoSalen in the presence or absence of oxygen were recorded as shown in Fig. 10. A band at 1205 cm^{-1} is clearly observed in the presence of oxygen. In contrast, it disappeared in the absence of oxygen. These changes are attributed to the nature of the reversible oxygenation of the Schiff base complexes of cobalt (Suzuki, Ishiguro, Kozuka & Nakamoto, 1981).

The catalytic activity of CS–CoSalen towards the electroreduction of dioxygen in aqueous solution was investigated with a cyclic voltammogram. The cyclic voltammogram curve obtained by slow scan (25 mV/s) of the modified electrode is shown in Fig. 8(2). The electrode had been exposed to air for 30 min before it was immersed in KCl solution (0.1 mol l^{-1}), which was saturated with N_2 for the measurement. There were hardly any peaks of oxidation occurring during the sweep. Two peaks of reduction at −0.23 and −0.67 V were observed. Moreover, with the repeated sweep, the peak current gradually decreased. This indicated clearly that oxygen in solution was irreversibly expended. As demonstrated earlier, the CS–CoSalen complex is a five-coordinate Co(II) complex in the absence of oxygen. The cobalt(II) ion is oxidized by oxygen in the presence of oxygen. The oxygenation products, thus, are structurally similar to a cobalt(III) complex. This suggests that the system can be viewed as a superoxide ion attached to cobalt(III), (Co(III)–O_2^-). It corresponds exactly to the oxidation peak ($Co^{II} \rightarrow Co^{III}$) at 0 V, which disappeared in the presence of oxygen. The six-coordinate superoxide cobalt(III) species in the presence of oxygen is more stable than the five-coordinate cobalt(III) species. The reduction peak of ($Co^{III} \rightarrow Co^{II}$) at −0.053 V for the five-coordinate complex thus shifts to −0.23 V for the six-coordinate complex. The reduction peak at −0.67 V is assigned to O_2^-, being irreversibly reduced because the current of this peak was related to the consumption of oxygen. The shapes of the cyclic voltammogram of the CS–CoSalen-modified electrode are dependent upon the scan rate. For the quick scan, the oxidation peak at 0 V appeared, even though oxygen was present, and the reduction peak at −0.67 V decreased. This dependence on scan rate could be interpreted by the competition between non-electrochemical and electrochemical reactions. There is ample time for reaction between the CS–Co(II)Salen with oxygen to form the CS–Co(III)Salen–O_2^- in a slow scan (25 mV/s). Thus, the oxidation peak at 0 V for the CS–Co(II)Salen CS–Co(III)-Salen disappeared, and the reduction peaks at −0.23 and −0.67 V appeared. In contrast, the major part of CS–Co(II)-Salen does not have enough time to react with oxygen in a quick scan (250 mV/s). Therefore, the oxidation peak at 0 V, naturally, appeared and the reduction peak at −0.67 V decreased due to decrease in the concentration of CS–CoSalen(III)O_2^-.

In addition, the effect of pH upon the electrochemical behavior was investigated. The reduction peak for O_2 is more obvious for the system at a lower pH (within a range of 7–10). This indicates that the proton present acts as a reactant of the reaction. The reduction product of oxygen was identified using a rotating ring–disk electrode modified by the CS–CoSalen. The current in the ring electrode was observed when the potential of the disk electrode reached −0.67 V, indicating that H_2O_2 is possibly produced. This tentative conclusion was further supported by the reaction of luminol, as a chemiluminescence phenomenon, with the solution of the electrochemical reaction of CS–Co(II)Salen–O_2^- that has been observed. This indicated that the

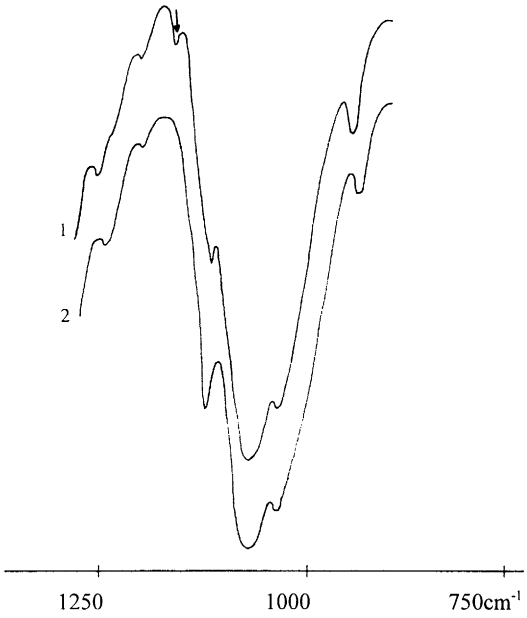

Fig. 10. IR spectra of CS–CoSalen obtained in the: (1) presence, and (2) absence of oxygen.

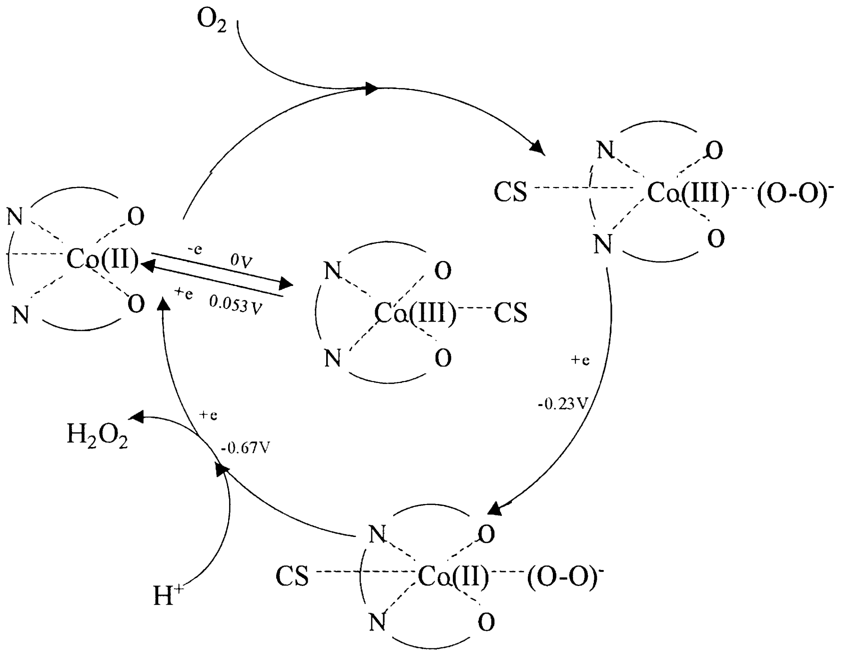

Fig. 11. Proposed electrochemical reaction mechanism.

solution produces H_2O_2. A proposed reaction mechanism is schematically shown in Fig. 11.

4. Conclusions

In this study, we showed that the CoSalen can be immobilized to CS through the coordination of amino groups in CS to the Co(II) in CoSalen. The CS–CoSalen binds molecular oxygen reversibly in the solid state through its vacant sixth coordination site to form a 1:1 ($Co:O_2$), superoxo complex. The immobilized complex may be used as a catalyst due to activation of molecular oxygen. The site isolation effect present in CS–CoSalen may inhibit the formation of dimers between two CoSalen molecules, and therefore promote the formation of six-coordinate species, CS–CoSalen(III)O_2^-. These results were further supported by electrochemical studies.

It may be concluded that immobilization prevents the formation of μ-oxo-dimers and other dimers. It is for this reason that the CS–CoSalen may possess a higher catalytic activity for the reactions of organic compounds with molecular oxygen.

Acknowledgements

We acknowledge financial support from the Natural Science Foundation of Shaanxi Province, People's Republic of China.

References

Bied-charreton, C., Frostin-rio, D., & Gaudemer, A. (1982). Synthesis and properties of polymeric Schiff bases and their Co(II), Cu(II) and Ni(II) complexes. *Journal of Molecular Catalysis*, *10*, 335–348.

Burness, J. H., Dillard, J. G., & Taylor, L. T. (1975). An X-ray photoelectron spectroscopic study of cobalt(II) Schiff base complexes and their oxygenation products. *Journal of the American Chemical Society*, *97* (21), 6080–6087.

Busetto, C., Cariati, F., & Fusi, A. (1973). Optically active complexes of Schiff bases II, complexes of cobalt(II) with tetradentate Schiff bases and their reactivity with oxygen. *Journal of the Chemical Society Dalton Transactions*, *7*, 754–756.

Dai, H., Li, J., & Han, Z. G. (1988). Synthesis and characterization of cobalt Schiff bases complexes and their oxygen adducts. *Journal of Inorganic Chemistry*, *4* (1), 61–67 (Chinese; CA 110:106973z).

Diemente, D., Hoffman, B. M., & Basolo, F. (1970). Electron paramagnetic resonance study of 1:1 cobalt–oxygen adducts. *Journal of the Chemical Society D*, *8*, 467–468.

Drago, R. S., Gaul, J., Zombec, A., & Strub, D. K. (1980). Preparation and catalytic oxidizing potential of polymer supported chelating aime and Schiff bases complexes. *Journal of the American Chemical Society*, *102*, 1033.

Ke, H. Zh., & Chen, Q. Ch. (1990). Potentiometric titration of chitosan by linear method. *Chemical Bulletin*, *10*, 44–46 (Chinese; CA 114:114416t).

Knorr, D. (1987). Recovery and utilization of chitin and chitosan in food processing waste management. *Food Technology*, 85–97.

Mark, J., Carter, D., Paul, R., & Fred, B. (1974). Oxygen carrier and redox properties of some neutral cobalt chelates, axial and in-plane ligand effects. *Journal of the American Chemical Society*, *96* (2), 392–400.

Matsujiro, S. (1980). ESR studies of axial ligation of low-spin cobalt(II) Schiff base complexes with Lewis bases and CO. *Bulletin of the Institute for Chemical Research Kyoto University*, *58* (2), 140–153.

Midorigaoka (1983). Highly deacetylated chitosan and its properties. *Journal of Applied Polymer Science*, *28*, 1909–1913.

Murray, K. S., Van den Bergen, A., & Kennedy, B. J. (1986). New insights into the electronic structures of solid-state dioxygen adducts of *N*,*N*′-ethylenebis(salicylaldiminato)cobalt(II), CoSalen, and of 'active' precursors. *Australian Journal of Chemistry*, *39* (9), 1479–1493.

Peniche-Covas, C., & Jimenez, M. S. (1988). Characterization of silver-binding chitosan by thermal analysis and electron impact mass spectroscopy. *Carbohydrate Polymers*, *9*, 249–256.

Rindone, B. (1985). Bis(salicylaldehyde)ethylenedi-iminecobalt(II) catalysed oxidation of aromatic amines with oxygen. *Journal of the Chemical Society Perkin Transactions II*, 1963–1967.

Robert, D. J., David, A. S., & Fred, B. (1979). Synthetic oxygen carriers related to biological systems. *American Chemical Society*, *79* (2), 139–179.

Ruzie, I. M., Smith, T. D., & Pilbrow, J. R. (1982). A study of substituent and base effect on the electron spin resonance spectra of the molecular oxygen adducts of cobalt(II) porphyrin chelates. *Journal of the Chemical Society Dalton Transactions*, 373–378.

Sakurada, M. (1980). ESR studies of axial ligation of low-spin Co(II) Schiff base complexes with Lewis bases and carbon monoxide. *Bulletin of the Institute for Chemical Research Kyoto University*, *52* (2), 140–153.

Smith, T. D., & Pilbrow, J. R. (1981). ESR of iron proteins. *Coordination Chemistry Reviews*, *39* (3), 295–383.

Suzuki, M., Ishiguro, T., Kozuka, M., & Nakamoto, K. (1981). Resonance Raman spectra, excitation profiles, and infrared spectra of $[Co(salen)]_2O_2$ in the solid state. *Inorganic Chemistry*, *20*, 1993–1996.

Tsuchida, E., Nishide, H., & Ohyanagi, M. (1987). ESR study on the species formed by reduction of iron(III) chelates of tetrasodium 3,10,17,24-tetrosulfontophthalocyanine in aqueous solution. *Macromolecules*, *20*, 1907–1912.

Yang, J. H., & Vigee, G. S. (1991). A cobalt complex immobilized to chitosan. *Journal of Inorganic Biochemistry*, *41*, 7–16.